Lagrangian Particle Trajectory Predictions in Turbulent Flows Using an Artificial Neural Network Algorithm

Lee Mortimer[1, a)] and Michael Fairweather[1, b)]

[1]*School of Chemical and Process Engineering, University of Leeds, Leeds LS2 9JT, United Kingdom*

[a)] *Corresponding author: l.f.mortimer@leeds.ac.uk*
[b)] *m.fairweather@leeds.ac.uk*

Abstract. An artificial neural network (ANN)-based hybrid machine learning algorithm used to predict Lagrangian particle trajectories is described and demonstrated within a turbulent channel flow. The algorithm is capable of predicting the response of trajectories to particle-fluid density ratios across a large range, representing calcite particles in water ($\rho_P^* = 2.5$) to air ($\rho_P^* = 2041.0$), highlighting its use across the scope of nuclear waste transportation flow systems. As well as the density ratio, the ANN uses the vertical location within the channel flow as its secondary feature variable. The ANN is trained on 10,000 simulated particle trajectories for each parameter set studied. Once suitably optimized, the ANN is shown to achieve around 6% mean-squared-error, with validation data sampled across three particle densities. Qualitative comparisons of trajectories demonstrate very good agreement at all three density ratios studied, though artefacts in the form of particle streaks arise due to the deterministic nature of the ANN. Investigation into the mean streamwise velocities suggests excellent agreement at low density ratios, and strong agreement at the upper bound of those studied, $\rho_P^* = 2041.0$. The normal stresses are shown to agree in the core of the channel, while weaker agreement is found towards the walls. The algorithm provides a strong foundation for obtaining accurate statistical quantities and further insights into wall-bounded turbulent particle-laden flows using both simulated and experimentally obtained trajectory datasets.

INTRODUCTION

The use of machine learning (ML) to augment analysis, prediction and decision making has received wide attention in recent years, forming a crucial part of both industrial and everyday processes such as medical imaging [1] and satellite navigation [2]. In such applications, ML relies upon the availability of labelled training data, such as magnetic resonance imaging scans for cancerous or non-cancerous growths, or routes across a city with associated distance costs. From these, models can be trained, and insights derived to make logical, optimized decisions and further to generate knowledge, working towards understanding the fundamentals of the system. In the field of particle-laden flows, the availability of high-fidelity training data is good, due to widely used simulation techniques such as Lagrangian particle tracking (LPT) [3], as well as experimental techniques such as particle imaging velocimetry [4]. In both cases, tens of thousands to millions of trajectories can be predicted or resolved, with techniques such as direct numerical simulation (DNS) or tracer particles further allowing for full resolution of the continuous phase. It is therefore clear that both single-phase and multi-phase fluid flows stand as suitable candidates for augmentation and analysis via ML. Due to this, the use of ML techniques has received recent attention in the fluid dynamics community, with challenges such as turbulence closure modelling [5] and flow process optimization [6] addressed.

For predicting the features of turbulent flows, various techniques have been demonstrated to date. For example, a random forest regression-based ML algorithm was used to predict the turbulence features in curved pipes using simulation data for training, which mapped the important characteristics of the flow, while slightly mispredicting the positions of additional vortices [7]. For particle-laden flows, the k-nearest neighbour algorithm has been used to recover the key fluid dynamic features of a mixing tank [8] and the radial mean velocity and concentration profiles in turbulent pipe flows [9], though the particle velocity fluctuations were not discussed. Artificial neural networks (ANNs) show further promise in such developments, capturing emergent phenomena such as preferential concentration [10]. The present work aims to utilize ANNs alongside leveraging dynamic training databases obtained through direct numerical simulation, to develop an algorithm capable of predicting particle trajectory responses to modification of the particle-fluid density ratio, recovering the key dynamic statistics, and greatly reducing the amount of time taken to obtain the particle behaviour features.

METHODOLOGY

The spectral-element method based DNS code, Nek5000 [11], is used to simulate the turbulent channel flow at shear Reynolds number, $Re_\tau = 180$, solving the Navier-Stokes equations in non-dimensional form numerically on a structured, discretized Cartesian grid comprising of 27 × 18 × 23 7th-order spectral elements, totalling approximately 3.9 million equivalent Gauss-Lobatto-Legendre (GLL) nodes. Variables such as the instantaneous velocity $\boldsymbol{u}_F$ and position $\boldsymbol{x}$ are non-dimensionalized by the bulk velocity U_B and the channel half-height, δ, respectively. The grid is scaled in the wall-normal direction of the channel flow (y) to distribute elements more densely closer to the wall, with uniform distribution in the streamwise (x) and spanwise (z) directions. The domain spans dimensions of $12\delta \times 2\delta \times 6\delta$, representing a classical turbulent channel flow. The flow is maintained by a constant pressure gradient $\partial p^*/\partial x^* = (Re_\tau/Re_B)^2$, with p^* the non-dimensional pressure, and Re_B the bulk Reynolds number. A Lagrangian particle tracking routine was developed and implemented, operating concurrently with Nek5000, in order to predict the trajectories of solid particles within the turbulent flow. Particles are represented as point-like impenetrable spheres. After each fluid timestep, the LPT solves the non-dimensional equations of motion for each particle, presented below:

$$\mathrm{M_{VM}}\frac{\partial \boldsymbol{u}_P^*}{\partial t^*} = \underbrace{\frac{3C_D|\boldsymbol{u}_S^*|}{4d_p^*\rho_P^*}\boldsymbol{u}_S^*}_{Drag} + \underbrace{\frac{3}{4}\frac{C_L}{\rho_P^*}(\boldsymbol{u}_S^* \times \boldsymbol{\omega}_F^*)}_{Lift} + \underbrace{\frac{1}{2\rho_P^*}\frac{D\boldsymbol{u}_F^*}{Dt^*}}_{Virtual\ Mass} + \underbrace{\frac{1}{\rho_P^*}\frac{D\boldsymbol{u}_F^*}{Dt^*}}_{Pressure\ Gradient} . \quad (1)$$

In Eq. (1), $\boldsymbol{u}_P^*$ is the instantaneous particle velocity vector, $\boldsymbol{u}_F^*$ is the instantaneous fluid velocity vector spectrally interpolated at the particle position, $\boldsymbol{u}_S^* = \boldsymbol{u}_F^* - \boldsymbol{u}_P^*$ is the slip velocity vector between the fluid and the particle, d_P^* is the non-dimensional particle diameter, ρ_P^* is the density ratio between the fluid and the particle and $\boldsymbol{\omega}_F^*$ is the fluid vorticity, given by $\boldsymbol{\omega}_F^* = \boldsymbol{\nabla} \times \boldsymbol{u}_F^*$. Finally, M_{VM} is the virtual mass modification term given by $M_{VM} = (1 + 1/2\rho_P^*)$. The drag coefficient, C_D, is calculated using $C_D = 24f_D/Re_P$, with $f_D = (1 + 0.15Re_P^{0.687})$ when $Re_P > 0.5$ and $f_D = 24/Re_P$ otherwise (in the Stokes regime). The term, Re_P is the particle Reynolds number, $Re_P = Re_B d_P^*|\boldsymbol{u}_S^*|$. Further details on the calculation and origins of these terms are fully described in [12]. The equations of motion are integrated utilizing a fourth-order accurate Runge-Kutta scheme, with a time step ($\Delta t^* = 0.005$) matching that of the continuous phase solver. Interactions between particles and the channel walls are resolved through elastic collision conditions. In the periodic directions (streamwise and spanwise), particles leaving through the boundary are reinjected at the corresponding location on the opposite side of the domain. Fluid and particle properties used to train the algorithm are presented in Table 1.

TABLE 1. Simulation properties used in training of hybrid ANN ML algorithm.

Parameter	Value		
Re_τ	180	180	180
ρ_P^*	2.5	1111.0	2041.0
d_P^*	0.0025	0.0025	0.0025
St^+	0.028	12.49	22.96
$N_{P,SIM}$	10,000	10,000	10,000

Trajectories are first generated using the simulation techniques presented above in accordance with Table 1. Each point in the trajectory is then pre-processed into a data array which consists of their vertical channel position, as well as their velocity components and mechanical parameters. The input feature and predictor arrays are assembled as $(y^*, Re_\tau, \rho_P^*, d_P^*)$ and $(u_{x,t}^*, u_{y,t}^*, u_{z,t}^*)$ respectively. The ANN is assembled with four input features, followed by three hidden layers containing 64, 32 and 16 neurons respectively with ReLU activation functions, followed by an output dense layer with three predicted values corresponding to the new particle velocity. The ANN is trained over 100 epochs and optimized using the adam optimizer, minimizing the mean-square-error (MSE) loss function, with a batch size of 32 and a train-test validation split of 0.3.

Once the ANN is trained, fictional particle trajectories may be generated by first initializing the position of all particles within the original boundaries of the channel flow, before assigning initial velocities based on the original local mean fluid velocity profile. The ANN hybrid ML algorithm is then performed such that subsequent velocities are predicted using $\boldsymbol{u}_{P,t+1} = \overline{\boldsymbol{u}}_{P,t} + \boldsymbol{u'}_F$. Here, $\overline{\boldsymbol{u}}_P$ is the predicted velocity generated using the ANN and $u'_F \sim \mathcal{N}(\mu, \sigma^2)$ comes from a validated Gaussian noise model based on the velocity fluctuations obtained from the DNS-LPT flow fields. Three variations of this term have been considered, with the first using the global channel fluid

velocity fluctuation distributions as performed in similar work [9]. The study also considered two potential improvements for resolving the fluctuations: one using the local fluid wall-normal distribution and a final one using the local particle wall-normal distribution, which are sampled *a priori*. The results presented in this paper use the latter, which demonstrated the strongest agreement. Particle positions are updated using a standard Euler time-stepping algorithm, with particle-wall collision detection and handling procedures identical to those present in the DNS-LPT.

RESULTS AND DISCUSSION

Initially, the ANN was trained on 10,000 particle trajectories for each density ratio dataset over 100 epochs, beyond which overfitting was observed, wherein the MSE exhibited an increase for the validation data. At around 100 epochs, the MSE in the validation data settled at around 6%. Figure 1 compares the particle trajectory histories between the DNS-LPT results and the ML-informed predictions. Visually, comparison of the streamwise velocities associated with the particles suggests confidence that particles close to the wall are accurately predicted to slow. Lateral motion seems more pronounced for the DNS predictions, with trajectories orientated transverse to the streamwise direction, though evidence of this is suggested for the ANN predictions. The ML model also tends to exhibit streaks of particles which likely represents particles starting close together upon injection being subject to similar further velocity predictions, an artefact of the determinism inherent in the ANN. This could likely be alleviated by dropout layers in which neurons are randomly deactivated, such that an essence of randomness is imparted on a prediction for a particular input feature vector, and will be pursued in further work.

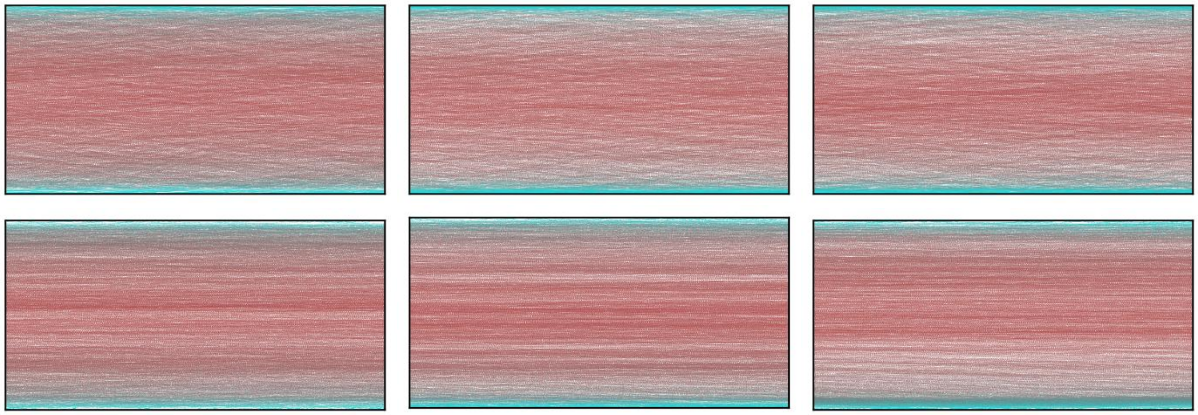

FIGURE 1. Particle trajectory histories in (x^*, y^*). Colour represents instantaneous particle streamwise velocity increasing from cyan to red. Left: $\rho_P^* = 2.5$, middle: $\rho_P^* = 1111.0$, right: $\rho_P^* = 2041.0$. Upper: DNS predictions, lower: ANN predictions.

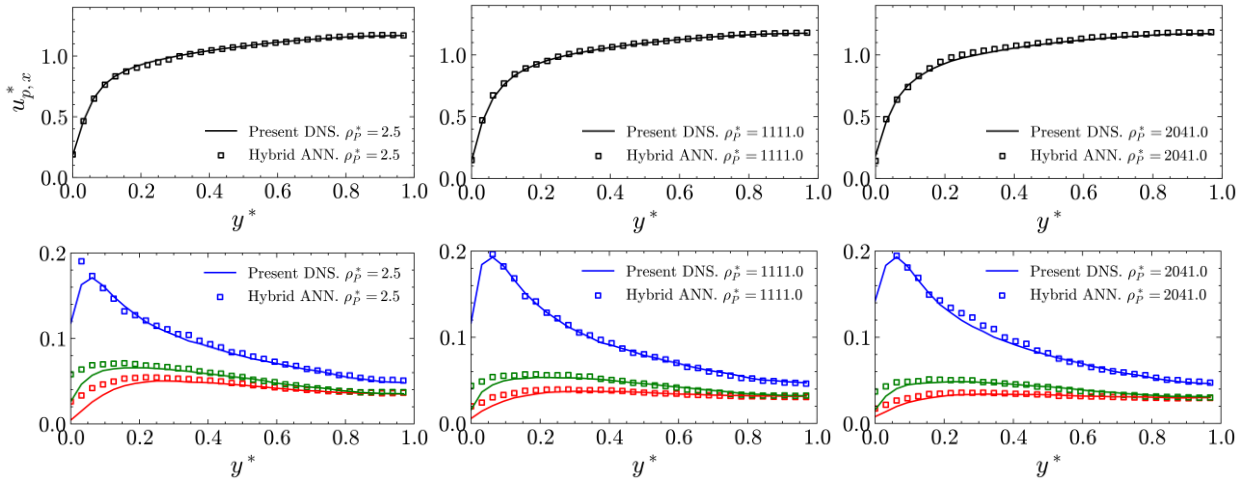

FIGURE 2. Comparison of particle phase mean streamwise velocity (upper) and root-mean-square (r.m.s.) of velocity fluctuations (lower). Left: $\rho_P^* = 2.5$, middle: $\rho_P^* = 1111.0$, right: $\rho_P^* = 2041.0$. Blue: $u_{x,RMS}'^*$, red: $u_{y,RMS}'^*$, green: $u_{z,RMS}'^*$.

Figure 2 presents a quantitative analysis of both the mean streamwise velocities (upper) and the r.m.s. of the velocity fluctuations (lower). For the two lower density ratios studied the agreement in the mean streamwise velocity is excellent, indicating that the ML predictions of particle velocity based on vertical position within the channel are accurate. For $\rho_P^* = 2041$, the hybrid ANN slightly overpredicts the velocities within the bulk of the channel, though the agreement is still good. The converse is true for the r.m.s. velocity fluctuation predictions, where the agreement is strong within the centre of the channel, and weaker in the turbulent regions, close to the wall. In these regions all components of the normal stresses tend to be overpredicted. This is likely due to the inability of the present technique to recover preferential concentration in low-speed streaks, which should be addressed in further improvements. That said, the technique is capable of performing with similar accuracy to DNS predictions for the first- and second- order particle statistics, with multiple orders of magnitude time reduction (around 4 minutes per simulation c.f. 48 hours).

CONCLUSIONS AND FURTHER WORK

The present study demonstrates an ANN-based predictive model used for generating particle trajectories in turbulent channel flows, trained on high-fidelity simulation data from DNS coupled with an LPT. Furthermore, by combining datasets across multiple density ratios (or Stokes numbers), the approach has been demonstrated to be well suited to capturing dynamic features across a range of material properties. Both qualitatively and quantitively the technique is shown to predict the mean streamwise velocities of particles within the flow correctly, when compared to equivalent DNS results. The normal stresses show best agreement in the channel core region, though weaker agreement close to the wall, where the fluctuations are overpredicted by the ANN technique, likely due to an inability to resolve motion within low-speed streaks.

The presented findings indicate that the use of ANN-based models offer significant promise for reducing computational costs, whilst maintaining high accuracy in predicting the motion of particles within turbulent channel flows. Aside from the reduction of three orders of magnitude in runtime, the technique also mostly recovers the correct fluctuation behaviour, a novelty to the present literature in this field. Further work should first include improvements to the model, with the incorporation of dropout layers to reduce determinism in identical input feature vectors. The present model also struggles to capture fully the particle behaviour in the turbulent regions and as such, more sophisticated models to account for turbophoresis and preferential concentration which combine the ANN with physics-informed techniques should be adopted.

ACKNOWLEDGMENTS

The authors are grateful to the UK Engineering and Physical Sciences Research Council for funding through the TRANSCEND (Transformative Science and Engineering for Nuclear Decommissioning) project (EP/S01019X/1), and Sellafield Ltd. for funding from the University of Leeds-Sellafield Ltd, Centre of Expertise for Sludge (Particulates & Fluids).

REFERENCES

1. I. Castiglioni, L. Rundo, M. Codari, G. Di Leo, C. Salvatore, M. Interlenghi, F. Gallivanone, A. Cozzi, N. C. D'Amico and F. Sardanelli, *Phys. Med.* **83**, 9-24 (2021).
2. A. Mohanty and G. Gao, EURASIP *J. Adv. Signal Process.* **2024**, 73 (2024).
3. J. G. M. Kuerten, *Flow Turbul. Combust.* **97**, 689-713 (2016).
4. M. R. Abdulwahab, Y. H. Ali, F. J. Habeeb, A. A. Borhana, A. M. Abdelrhman and S. M. A. Al-Obaidi, *J. Adv. Res. Fluid Mech. Therm. Sci.* ***65***, 213-229 (2020).
5. L. Zhu, W. Zhang, X. Sun, Y. Liu and X. Yuan, *Aerosp. Sci. Technol.* **110**, 106452 (2021).
6. A. D. Clayton, A. M. Schweidtmann, G. Clemens, J. A. Manson, C. J. Taylor, C. G. Niño, T. W. Chamberlain, N. Kapur, A. J. Blacker, A. A. Lapkin and R. A. Bourne, *Chem. Eng. J.* **384**, 123340 (2020).
7. P. Jain, A. Choudhury, P. Dutta, K. Kalita and P. Barsocchi, *Processes* **9**, 2095 (2021).
8. K. Li, C. Savari, H. A. Sheikh and M. Barigou, *Phys. Fluids* **35**, 015150 (2023).
9. Z. Yang, K. Li and M. Barigou, *Phys. Fluids* **35**, 113309 (2023).
10. J. Hu, Z. Lu and Y. Yang, *Phys. Rev. Fluids* **9**, 034606 (2024).
11. P. F. Fischer, J. W. Lottes and S. G. Kerkemeier, Nek5000, available at: http://nek5000.mcs.anl.gov/; accessed September 1, 2008.
12. L. F. Mortimer, D. O. Njobuenwu and M. Fairweather, *Phys. Fluids* **31**, 063302 (2019).